



## Analysis of generalized Flip, Chenciner, and Resonance bifurcations in a discrete predator-prey system

Javad Hadadi<sup>1</sup>, Zohreh Eskandari<sup>2,\*</sup> and Reza Khoshsiar Ghaziani<sup>1</sup>

<sup>1</sup>Department of Mathematical Sciences, Shahrekord University, Shahrekord, Iran.

<sup>2</sup>Department of Mathematics, Faculty of Science, Fasa University, Fasa, Iran.

### Abstract

In this study, we investigate codimension-two bifurcations in a discrete predator-prey model. First, we provide a theoretical analysis of several bifurcation types, including 1:2, 1:3, and 1:4 resonances, generalized flip bifurcations, and generalized Neimark-Sacker bifurcations. Using the center manifold theory and normal form reduction, the conditions for the occurrence of these bifurcations are derived. Subsequently, numerical simulations are performed with the `MatcontM` package in MATLAB to validate the analytical results. The findings offer a comprehensive view of the complex dynamics arising from codimension-two bifurcations in biological interaction systems.

**Keywords.** Predator-prey model, Generalized flip bifurcation, Chenciner bifurcation, Resonance 1:2, 1:3, 1:4, `matcontm`.

**2010 Mathematics Subject Classification.** 37L10, 37M20, 39A28, 65P30.

### 1. INTRODUCTION

Discrete-time predator-prey models play a fundamental role in understanding population dynamics in ecological systems, particularly when species exhibit non-overlapping generations or seasonal reproduction patterns. In contrast to continuous-time models, discrete systems are capable of exhibiting a broader range of dynamical behaviors such as period-doubling cascades, quasi-periodicity, and chaos even with relatively simple nonlinear structures. Consequently, discrete predator-prey frameworks have attracted increasing attention in the study of complex biological interactions and nonlinear phenomena in recent years [2, 11].

One of the most significant aspects of discrete dynamical systems is the occurrence of bifurcations as system parameters vary. Bifurcation theory provides a systematic methodology for classifying qualitative changes in system behavior and has become a cornerstone in the analysis of nonlinear models. In ecological modeling, bifurcations typically correspond to important biological transitions such as population extinction, oscillatory outbreaks, or coexistence loss [8, 12]. Among these phenomena, codimension-one bifurcations such as flip and Neimark-Sacker bifurcations have been extensively studied and are known to generate periodic and quasi-periodic dynamics in predator-prey systems [9].

However, codimension-two bifurcations represent a higher level of dynamical complexity, arising when two independent bifurcation conditions are simultaneously satisfied. These bifurcations serve as organizing centers in parameter space and are responsible for interactions between multiple local bifurcation mechanisms. Typical examples include strong resonance bifurcations (1:2, 1:3, and 1:4), generalized flip (degenerate period-doubling) bifurcations, and generalized Neimark-Sacker (Chenciner) bifurcations [6, 9, 13]. The local dynamics near these points often involve complicated structures such as invariant tori, Arnold tongues, and multi-stability, making their theoretical investigation both challenging and essential.

In recent decades, normal form theory and center manifold reductions have become indispensable analytical tools for studying bifurcations in nonlinear systems. These techniques enable dimensional reduction and provide simplified

Received: 16 December 2025; Accepted: 27 June 2026.

\* Corresponding author. Email: z-eskandari@fasau.ac.ir .

equations that preserve the essential dynamics near critical points [3, 7]. Moreover, Lyapunov coefficients derived from normal forms play a central role in determining the direction and stability of emerging invariant sets, such as periodic orbits and quasi-periodic solutions.

Although codimension-two bifurcations in continuous predator–prey systems have been widely documented, corresponding results for discrete ecological models remain relatively limited. Existing literature mainly focuses on codimension-one scenarios, while detailed classification and numerical verification of codimension-two phenomena in discrete predator–prey models is still inadequate [2, 4]. Furthermore, due to strong nonlinear interactions, purely analytical results are often insufficient to fully describe local dynamics, which motivates the integration of numerical continuation techniques.

In this study, we conduct a comprehensive analysis of codimension-two bifurcations in a two-dimensional discrete predator–prey model. Using center manifold theory and normal form analysis, we derive analytical conditions for the existence of resonance bifurcations (1:2, 1:3, 1:4), generalized flip bifurcations, and generalized Neimark–Sacker bifurcations. Numerical simulations are performed using the MATLAB package `MatcontM`, which allows for accurate continuation and detection of bifurcation points in discrete maps [5]. The combined theoretical and numerical framework provides deeper insight into the global dynamic structures arising from local degeneracies and offers a rigorous foundation for understanding complex biological oscillations driven by parameter interactions.

The results presented in this paper contribute to the growing body of research on nonlinear discrete ecological models and highlight the significance of codimension-two bifurcation analysis in understanding ecological resilience, instability, and pattern formation.

## 2. MODEL FORMULATION

The discrete predator-prey system under consideration ( $X \mapsto f(X)$ ) is given by

$$\begin{cases} x_{n+1} = ax_n(1 - x_n) - cx_ny_n, \\ y_{n+1} = by_n(1 - y_n) + dx_ny_n, \end{cases} \quad (2.1)$$

where all parameters are positive and their biological interpretation can be found in [1]. Here  $a$  and  $b$  are the intrinsic growth rates of prey and predator,  $c$  the predation rate, and  $d$  the conversion efficiency. To study codimension-two bifurcations, we first compute the equilibrium points:

$$\begin{cases} ax(1 - x) - cxy = 0, \\ by(1 - y) + dxy = 0. \end{cases}$$

Thus, the equilibria are

$$\begin{aligned} X_0 &= (0, 0), & X_1 &= \left(0, \frac{b-1}{b}\right), & X_2 &= \left(\frac{a-1}{a}, 0\right), \\ X_3 &= \left(\frac{ba - bc - b + c}{ba + cd}, \frac{ba + ad - a - d}{ba + cd}\right). \end{aligned}$$

Using the center manifold reduction, the normal forms associated with these bifurcations are derived [9, 10], and numerical simulations with `matcontm` confirm the analytical findings.

## 3. ANALYSIS OF CODIMENSION-TWO BIFURCATIONS

To investigate codimension-two bifurcations in detail, it is necessary to analyze not only the location of equilibrium points but also the local behavior of the system in their neighborhoods. The Jacobian matrix of the system at an equilibrium point  $X$  is given by

$$J(X) = \begin{pmatrix} a(1 - 2x) - cy & -cx \\ dy & b(1 - 2y) + dx \end{pmatrix}.$$



By substituting the coordinates of the equilibria  $X_0, X_1, X_2, X_3$  into this matrix, the characteristic equation and eigenvalues are obtained, which provide the conditions for the occurrence of codimension-two bifurcations.

For each equilibrium point  $X_* = (x_*, y_*)$ , the characteristic polynomial is derived from  $\det(\lambda I - J) = 0$  and can be written as

$$\lambda^2 - \text{tr}(J)\lambda + \det(J) = 0,$$

where the trace and determinant of the Jacobian are

$$\text{tr}(J) = a(1 - 2x_*) - cy_* + b(1 - 2y_*) + dx_*,$$

$$\det(J) = (a(1 - 2x_*) - cy_*)(b(1 - 2y_*) + dx_*) + cdx_*y_*.$$

If  $x_* > 0$  and  $y_* > 0$ , the equilibrium conditions

$$a(1 - x_*) = cy_*, \quad b(1 - y_*) = -dx_*$$

imply that

$$\text{tr}(J) = -b - (a + d)x_*, \quad \det(J) = ax_*(b + d).$$

Thus, the characteristic equation at the interior equilibrium takes the compact form

$$\lambda^2 + (b + (a + d)x_*)\lambda + ax_*(b + d) = 0.$$

#### 4. BIFURCATIONS AT THE EQUILIBRIUM $X_3$

We now focus on codimension-two bifurcations occurring at the interior equilibrium  $X_3$ .

**4.1. Generalized Neimark–Sacker Bifurcation.** We first consider the Neimark–Sacker bifurcation. To obtain the generalized case, the first Lyapunov coefficient is set to zero. If

$$\det(J) = 1, \quad \text{tr}(J)^2 - 4 < 0,$$

the conditions for a Neimark-Sacker bifurcation are satisfied. In particular, at  $X_3$  the bifurcation occurs when

$$d = -\frac{a(ab^2 - b^2c - 2ba - 2b^2 + 3bc + 3b - 2c)}{a^2b - abc - 3ba + ac + bc + 2b - c}.$$

The reduced system on the center manifold takes the form [10]

$$\zeta \mapsto \zeta e^{i\theta_0} (1 + d_{NS}|\zeta|^2) + \mathcal{O}(|\zeta|^4), \quad \zeta \in \mathbb{C}, \quad e^{im_0\theta_0} \neq 1 \quad (m_0 = 1, 2, 3, 4),$$

where the coefficient  $d_{NS}$  is given by

$$d_{NS} = \frac{1}{2} e^{-i\theta_0} \langle \eta, 2H(\mu, (I_n - J)^{-1}H(\mu, \bar{\mu})) + H(\bar{\mu}, (e^{2i\theta_0}I_n - J)^{-1}H(\mu, \bar{\mu})) \rangle.$$

Here  $\mu$  and  $\eta$  denote the normalized right and left eigenvectors, respectively

$$\mu_1 = \left[ 1 \quad -\frac{a(e^{2i\theta}b + ((2a-c-4)b+c)e^{\theta_1} + ((a-c-2)b+c)(a-2))}{c(e^{2i\theta}c + ((a-1)b-2c)e^{\theta_1} + (a-1)(a-c-2)b+ac)} \right]^T,$$

$$\bar{\eta}_1 = \left[ 1 \quad \frac{((a-1)b-2c)e^{-i\theta} + e^{-2i\theta}c + (a-1)(a-c-2)b+ac}{a((b-3)e^{-i\theta} - b + e^{-2i\theta} + 2)} \right]^T,$$

$$\mu = \frac{\mu_1}{\sqrt{\langle \mu_1, \mu_1 \rangle}}, \quad \eta = \frac{\eta_1}{\langle \eta_1, \mu \rangle},$$

and  $H(x, y)$  represents the quadratic terms of the nonlinear mapping

$$H_i(x, y) = \sum_{j,k=1}^n \frac{\partial^2 f_i(X_3)}{\partial \varepsilon_j \partial \varepsilon_k} x_j y_k = \begin{bmatrix} -2ax_1y_1 - cx_1y_2 - cx_2y_1 \\ -2bx_2y_2 + dx_1y_2 + dx_2y_1 \end{bmatrix}.$$

If  $\Re(d_{NS}) < 0$ , the bifurcation is supercritical; if  $\Re(d_{NS}) > 0$ , it is subcritical; and if  $\Re(d_{NS}) = 0$ , a generalized Neimark–Sacker bifurcation occurs. In this case, the reduced system becomes

$$\zeta \mapsto \zeta e^{i\theta_0} + a_1\zeta|\zeta|^2 + a_2\zeta|\zeta|^4 + \mathcal{O}(|\zeta|^6), \quad \zeta \in \mathbb{C},$$



where  $a_1$  and  $a_2$  are obtained from higher-order normal form computations

$$\begin{aligned} a_1 &= \langle \eta, 2H(\mu, (I_n - J)^{-1}H(\mu, \bar{\mu})) + H(\bar{\mu}, (e^{2i\theta_0}I_n - J)^{-1}H(\mu, \bar{\mu})) \rangle, \\ a_2 &= \frac{1}{12} \langle \eta, 3H(h_{20}, h_{12}) + 6H(h_{11}, h_{21}) + 3H(\mu, h_{22}) + H(h_{02}, h_{30}) + 2H(\bar{\mu}, h_{31}) \rangle, \end{aligned}$$

where  $h_{20} = \bar{h}_{02}, h_{12} = \bar{h}_{21}, h_{11}, h_{22}, h_{30}, h_{31}$  are obtained as follows:

$$\begin{aligned} (J - e^{2i\theta_0}I_n)h_{20} &= -H(\mu, \mu), \\ (J - I_n)h_{11} &= -H(\mu, \bar{\mu}), \\ (J - e^{3i\theta_0}I_n)h_{30} &= -3H(\mu, h_{20}), \\ (J - e^{i\theta_0}I_n)h_{21} &= 2c_1^0\mu - H(\bar{\mu}, h_{20}) - 2H(\mu, h_{11}), \\ (J - e^{2i\theta_0}I_n)h_{31} &= -\left[3H(\mu, h_{21}) + 3H(h_{11}, h_{20}) + H(\bar{\mu}, h_{30})\right] + 3a_1h_{20}e^{i\theta_0}, \\ (J - I_n)h_{22} &= -\left[H(h_{20}, h_{02}) + 2H(h_{11}, h_{11}) + 2H(\mu, h_{12}) + 2H(\bar{\mu}, h_{21})\right] + 2h_{11}(a_1e^{-i\theta_0} + \bar{a}_1e^{i\theta_0}). \end{aligned}$$

If the second Lyapunov coefficient

$$L_2 = \Re(e^{-i\theta_0}a_2) + \frac{1}{2}(\Im(e^{-i\theta_0}a_1))^2,$$

is nonzero, the non-degeneracy condition holds and the generalized Neimark–Sacker bifurcation is confirmed.

**4.2. Generalized Flip Bifurcation.** Next, we consider the flip bifurcation. If  $\lambda = -1$  is an eigenvalue of the Jacobian and no other eigenvalue lies on the unit circle, a flip bifurcation may occur at  $X_3$ . The condition is satisfied when

$$d = -\frac{a(ab^2 - b^2c - 3ba - 3b^2 + 4bc + 9b - 3c)}{a^2b - abc - 4ba + ac + bc + 3b + 3c}.$$

The reduced system on the center manifold is [10]

$$w \mapsto -w + b_{flip}w^3 + \mathcal{O}(w^4), \quad w \in \mathbb{R},$$

where

$$b_{flip} = \frac{1}{6} \langle \eta, 3H(\mu, (I_n - J)^{-1}H(\mu, \mu)) \rangle,$$

and the left and right eigenvectors are obtained as follows:

$$\begin{aligned} \mu_1 &= \left[ \begin{array}{c} -\frac{c((a-1)(a-c-3)b + c(a+3))}{a(a-3)((a-c-3)b+c)} \\ 1 \end{array} \right]^T, \\ \eta_1 &= \left[ \begin{array}{c} 1 \\ -\frac{a^2b - abc - 4ab + ac + bc + 3b + 3c}{(2b-6)a} \end{array} \right]^T, \\ \mu &= \frac{\mu_1}{\sqrt{\langle \mu_1, \mu_1 \rangle}}, \quad \eta = \frac{\eta_1}{\langle \eta_1, \mu \rangle}. \end{aligned}$$

If  $b_{flip} > 0$ , the bifurcation is supercritical; if  $b_{flip} < 0$ , it is subcritical; and if  $b_{flip} = 0$ , a generalized flip bifurcation occurs. In this case, the reduced system becomes

$$w \mapsto -w + c_{gflip}w^5 + \mathcal{O}(w^6), \quad w \in \mathbb{R},$$

where

$$c_{gflip} = \frac{1}{120} \langle \eta, 5H(\mu, h_4) + 10H(h_2, h_3) \rangle,$$



with  $h_2, h_3, h_4$  obtained from higher-order expansions

$$\begin{aligned} h_2 &= (I_n - J)^{-1}H(\mu, \mu), & h_3 &= -3(I_n + J)^{-1}H(\mu, h_2), \\ h_4 &= (I_n - J)^{-1}(4H(\mu, h_3) + 3H(h_2, h_2)). \end{aligned}$$

**4.3. Resonance 1:3.** In the Neimark–Sacker bifurcation, if  $\theta_0 = \pm 2\pi/3$ , a 1:3 resonance may occur. Hence, we have

$$\begin{aligned} d &= \frac{(7a^2 - 9ac + 3c^2 - 35a + 21c + 49)a}{(4a - 3c - 7)(a^2 - ac - 5a + 4c + 7)}, \\ b &= -\frac{c(a - 7)}{a^2 - ac - 5a + 4c + 7}. \end{aligned}$$

The reduced system on the center manifold is [10]

$$w \mapsto e^{\pm \frac{2\pi}{3}i} w + b_0 \bar{w}^2 + c_0 w |w|^2 + \mathcal{O}(|w|^4), \quad w \in \mathbb{C},$$

where

$$\begin{aligned} b_0 &= \frac{1}{2} \langle \eta, H(\bar{\mu}, \bar{\mu}) \rangle, \\ c_0 &= \frac{1}{2} \left\langle \eta, 2H(\mu, (I_n - J)^{-1}H(\mu, \bar{\mu})) - H(\bar{\mu}, (e^{2i\theta_0} I_n - J)^{-1}(2\bar{b}_0 \bar{\mu} - H(\mu, \mu))) \right\rangle. \end{aligned}$$

The stability of the resulting cycle is determined by the sign of

$$a_2(0) = \Re \left( \frac{e^{-i\theta_0} c_0}{|b_0|^2} - 1 \right).$$

**4.4. Resonance 1:4.** In the Neimark–Sacker bifurcation, if  $\theta_0 = \pm \pi/2$ , a 1:4 resonance may occur. Hence, we have

$$\begin{aligned} d &= \frac{(5a^2 - 6ac + 2c^2 - 20a + 10c + 25)a}{(3a - 2c - 5)(a^2 - ac - 4a + 3c + 5)}, \\ b &= -\frac{c(a - 5)}{a^2 - ac - 4a + 3c + 5}. \end{aligned}$$

The reduced system on the center manifold is given by [10]

$$w \mapsto iw + c_0 w |w|^2 + d_0 \bar{w}^3 + \mathcal{O}(|w|^4), \quad w \in \mathbb{C},$$

where the normal form coefficients are obtained as

$$\begin{aligned} c_0 &= \frac{1}{2} \langle \eta, 2H(\mu, (I_n - A)^{-1}H(\mu, \bar{\mu})) - H(\bar{\mu}, (I_n + J)^{-1}H(\mu, \mu)) \rangle, \\ d_0 &= \frac{1}{6} \langle \eta, -3H(\bar{\mu}, (I_n + A)^{-1}H(\bar{\mu}, \bar{\mu})) \rangle. \end{aligned}$$

The bifurcation scenario near the resonance point is determined by

$$A_0 = \frac{-ic_0}{|d_0|}.$$

**4.5. Resonance 1:2.** If the system has two eigenvalues equal to  $-1$ , and the following conditions hold:

$$\begin{aligned} d &= \frac{(9a^2 - 12ac + 4c^2 - 54a + 36c + 81)a}{(5a - 4c - 9)(a^2 - ac - 6a + 5c + 9)}, \\ b &= -\frac{c(a - 9)}{a^2 - ac - 6a + 5c + 9}, \end{aligned}$$

then a 1:2 resonance bifurcation occurs. The reduced system on the center manifold is [10]

$$\begin{pmatrix} w_1 \\ w_2 \end{pmatrix} \mapsto \begin{pmatrix} -w_1 + w_2 \\ -w_2 + c_0 w_1^3 + d_0 w_1^2 w_2 \end{pmatrix} + \mathcal{O}(\|w\|^4), \quad w \in \mathbb{R}^2,$$



where the normal form coefficients are

$$c_0 = \frac{1}{2} \langle \eta_0, H(\mu_0, (I - J)^{-1} H(\mu_0, \mu_0)) \rangle,$$

$$d_0 = \frac{1}{2} \left[ \langle \eta_0, 2H(\mu_0, h_{11}) + H(\mu_1, h_{20}) \rangle \right] + \frac{1}{2} \left[ \langle \eta_1, 3H(\mu_0, h_{20}) \rangle \right],$$

with  $h_{11}$  and  $h_{20}$  determined by

$$(J - I_n)h_{20} = -H(\mu_0, \mu_0), \quad (J - I_n)h_{11} = -H(\mu_0, \mu_1) - h_{20},$$

and for the left and right eigenvectors we have:

$$\mu_0 = \begin{pmatrix} -\frac{c(5a-4c-9)}{a(3a-2c-9)} \\ 1 \end{pmatrix},$$

$$\mu_1 = \begin{pmatrix} \frac{c^3(5a-4c-9)^3(a-c)}{a(4a^4-4a^3c+26a^2c^2-40a^2c^2-40ac^3+16c^4-36a^3+18a^2c-90ac^2+72c^3+81a^2+81c^2)(3a-2c-9)^2} \\ -\frac{(5a-4c-9)^2c^2(2a-c-9)(a-c)}{(4a^4-4a^3c+26a^2c^2-40a^2c^2-40ac^3+16c^4-36a^3+18a^2c-90ac^2+72c^3+81a^2+81c^2)(3a-2c-9)^2} \end{pmatrix},$$

$$\eta_0 = \begin{pmatrix} \frac{a(4a^4-4a^3c+26a^2c^2-40ac^3+16c^4-36a^3+18a^2c-90ac^2+72c^3+81a^2+81c^2)(3a-2c-9)^3}{c^3(5a-4c-9)^3(a-c)^2} \\ \frac{(4a^4-4a^3c+26a^2c^2-40ac^3+16c^4-36a^3+18a^2c-90ac^2+72c^3+81a^2+81c^2)(3a-2c-9)^2}{c^2(5a-4c-9)^2(a-c)^2} \end{pmatrix},$$

$$\eta_1 = \begin{pmatrix} \frac{(3a-2c-9)a(2a-c-9)}{(a-c)c(5a-4c-9)} \\ \frac{3a-2c-9}{a-c} \end{pmatrix},$$

where

$$\langle \eta_0, \mu_1 \rangle = \langle \eta_1, \mu_0 \rangle = 1,$$

$$\langle \eta_0, \mu_0 \rangle = \langle \eta_1, \mu_1 \rangle = 0.$$

## 5. NUMERICAL SIMULATIONS

We now perform numerical simulations using the MATLAB package `matcontm` [5]. First, fixing

$$a = 2.8960264, \quad c = 0.05, \quad b = 2.5,$$

and varying  $d$ , we observe that at  $d = 1$  a supercritical Neimark–Sacker bifurcation occurs with first Lyapunov coefficient  $\Re(d_{NS}) = -7.0026$  at the fixed point  $X_3 = (0.63992096, 0.85596835)$ . A flip bifurcation with normal form coefficient  $b_{flip} = -9.4784$  occurs at  $X_3 = (0.63941747, 0.88513029)$  for  $d = 1.1148049$ , (see Figures 1 and 3(e)).

When parameters  $b$  and  $d$  are varied near the Neimark-Sacker bifurcation, resonances 1:2, 1:3, and 1:4 are observed. Similarly, near the flip bifurcation, varying  $b$  and  $d$  leads to the generalized flip bifurcation (see Figures 2, 3(f), 4, and 5).

For example:

- At  $b = 2.6308146$ ,  $d = 0.80221889$ , the 1:2 resonance occurs at  $X_3 = (0.6406242, 0.81523625)$  with normal form coefficients  $[c, d] = -2.61949961, -3.1194 \times 10^1$  (Figure 3(f)).
- At  $b = 0.21329635$ ,  $d = 4.1427429$ , the 1:3 resonance occurs at  $X_3 = (0.53797809, 6.7605529)$  with  $\Re(c_1) = -1.0655$  (Figure 4(g)).
- At  $b = 0.058183117$ ,  $d = 3.8616137$ , the 1:4 resonance occurs at  $X_3 = (0.43533199, 12.705869)$  with  $A_0 = -4.0297 - 2.7222i$  (Figure 4(h)).
- At  $b = 1.8137753$ ,  $d = 3.355786$ , the generalized flip bifurcation occurs at  $X_3 = (0.62692703, 1.6085831)$  with  $c_{gflip} = -1.8710$ .

Finally, fixing  $a = 7.6415392$ ,  $c = 20.961481$ , and varying  $b$  and  $d$ , we find that at  $b = 1.3346622$ ,  $d = 3.75$ , a generalized Neimark–Sacker bifurcation occurs at  $X_3 = (0.020823, 0.309253)$  with second Lyapunov coefficient  $L_2 = 5.5350 \times 10^3$  (Figure 5). Resonances 1:3 and 1:4 are also observed under parameter variations (Figure 2(d)).



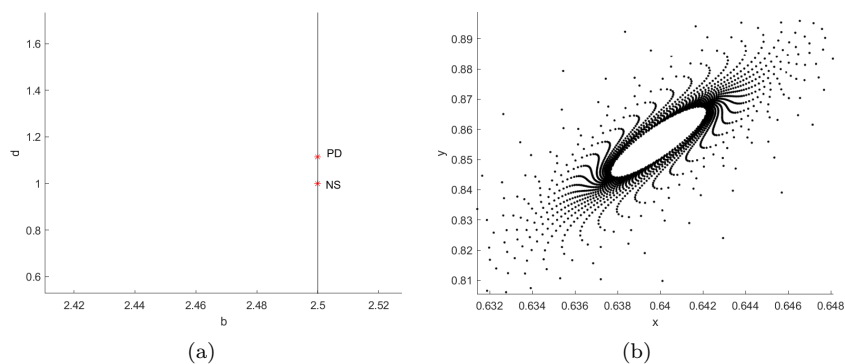


FIGURE 1. (a) Diagram of codimension-one bifurcations in the system. (b) A stable closed invariant curve emerging from a Neimark-Sacker bifurcation

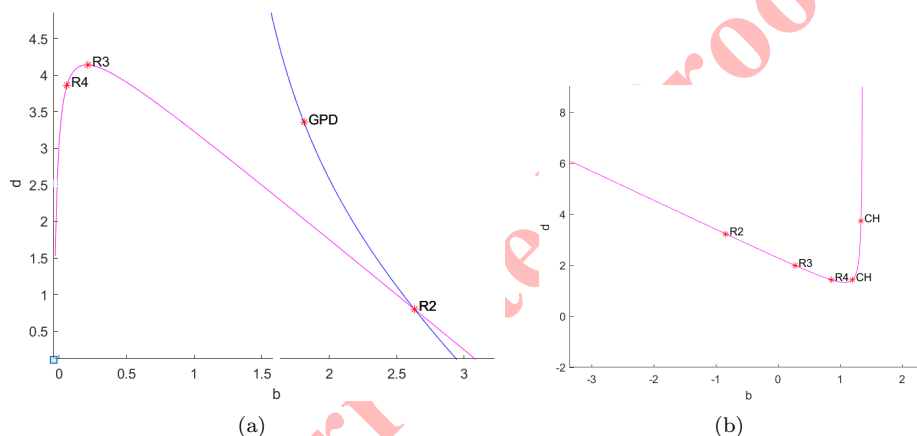


FIGURE 2. (a) The pink and blue curves represent the Neimark-Sacker and flip bifurcations, respectively. (b) Generalized Neimark-Sacker bifurcation and other codimension-two bifurcations in the Neimark-Sacker bifurcation curve.

## 6. ECOLOGICAL IMPLICATIONS

Each bifurcation has a concrete meaning for real predator and prey populations. In this section, we translate the mathematical results into ecological language.

**6.1. 1:2 resonance (period-2 behavior).** A 1:2 resonance produces a stable two step cycle. High prey leads to high predators, then both crash and the pattern repeats. Such two year cycles are common in arctic species like lemmings and voles. This resonance opens the door to period doubling and chaos. Near this bifurcation, a small environmental change can push the system into wild fluctuations.

**6.2. 1:3 resonance (period-3 behavior).** A 1:3 resonance produces a three step cycle. By the Li Yorke theorem, period three implies chaos. In real systems, three year cycles appear in some insect populations and rodent plague systems, with outbreaks followed by sharp declines. For wildlife managers, this resonance warns that the population may be hard to predict.



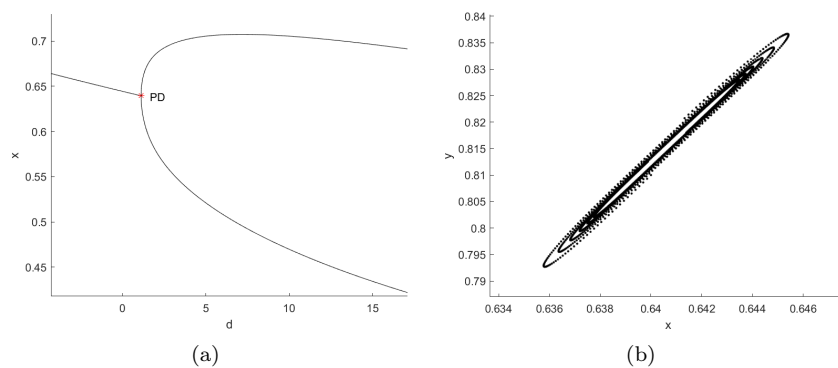


FIGURE 3. (a) Flip bifurcation diagram. (b) Phase portrait for the 1:2 resonance bifurcation.

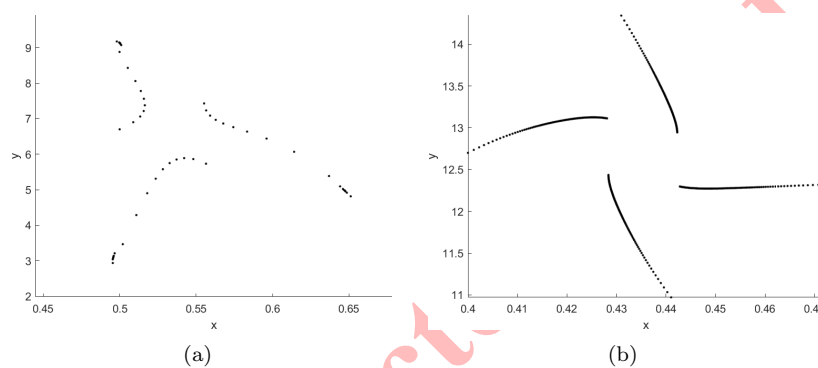


FIGURE 4. (g) Phase portrait for the 1:3 resonance bifurcation. (h) Phase portrait for the 1:4 resonance bifurcation.

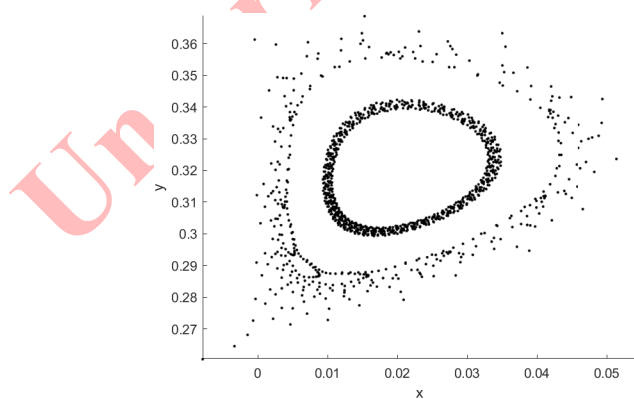


FIGURE 5. Phase portrait for the generalized Neimark-Sacker bifurcation.

**6.3. 1:4 resonance (period-4 behavior).** A 1:4 resonance produces a four step cycle, more complex than two or three step cycles. Four year cycles are well known in snowshoe hares and lynx in northern Canada. Near this bifurcation, multistability often occurs: multiple attractors coexist, so the final outcome depends on initial conditions. Biologists call this history matters.

**6.4. Generalized Neimark Sacker bifurcation.** Unlike periodic resonances, this bifurcation gives quasiperiodic oscillations. Populations fluctuate in an almost regular but never exactly repeating pattern. They remain bounded and do not go extinct, but their future cannot be predicted exactly. Ecologically, this means stable coexistence with ongoing irregular fluctuations. The generalized version is more complex: a stable equilibrium may coexist with an invariant cycle, and small environmental changes can cause sudden shifts between them. This can appear as an unexpected collapse or outbreak with no obvious external cause.

**6.5. Biological plausibility of the parameter values.** The parameter values we use are biologically realistic. For example, on page 7 we have  $b = 0.058$  and  $d = 3.86$ . A prey growth rate  $b$  around 0.05 to 0.1 is realistic for slowly reproducing species like large mammals or birds. A conversion efficiency  $d$  between 2 and 5 may seem high, but it occurs when a predator consumes large amounts of prey per unit of its own biomass. In many aquatic systems, zooplankton convert a significant fraction of ingested algae into their own biomass. More generally, our parameter values for all resonances fall within ranges reported in empirical studies. Thus, the dynamical behaviors we describe could in principle be observed in real ecosystems.

**6.6. Implications for management and conservation.** Knowing bifurcation thresholds helps anticipate ecological shifts. A system may move from stable coexistence to cycles, from cycles to chaos, or from coexistence to extinction.

1:2 resonance. Warns of two year cycles and a possible period doubling route to chaos.

1:3 resonance. Period three implies chaos in nearby parameter ranges.

1:4 resonance. Suggests four year cycles and multiple stable states where history matters.

Generalized Neimark Sacker bifurcation. Small perturbations can push the system into quasiperiodic and unpredictable fluctuations.

If a real predator prey system operates near these bifurcations, small management interventions such as habitat restoration, limited predator culling, or supplementary feeding may restore stable coexistence. Ignoring these thresholds could lead to sudden surprises.

In short, these bifurcations describe concrete mechanisms by which predator prey interactions generate cycles, outbreaks, multi year fluctuations, and loss of coexistence. Future empirical work should test these predictions by fitting the model to real data and comparing observed dynamics with our bifurcation diagrams.

## 7. CONCLUSION

In this work, we conducted a comprehensive study of codimension-two bifurcations in a discrete predator-prey system. By combining analytical techniques such as center manifold reduction and normal form theory with numerical simulations using the MATLAB package `matcontm`, we identified and characterized several bifurcation scenarios, including generalized Neimark-Sacker and flip bifurcations, as well as 1:2, 1:3, and 1:4 resonances.

The analytical results provided explicit conditions for the occurrence of these bifurcations, while the numerical experiments confirmed their validity and illustrated the rich dynamical behaviors that emerge near critical parameter values. Our findings highlight the crucial role of codimension-two bifurcations in shaping complex oscillatory patterns and nonlinear dynamics in ecological interaction models.

This study not only deepens the theoretical understanding of bifurcation phenomena in discrete biological systems but also demonstrates the effectiveness of combining rigorous mathematical analysis with computational tools. Future research may extend these methods to higher-dimensional systems or explore the implications of such bifurcations in applied contexts such as population management, epidemiology, and ecosystem stability.

## REFERENCES

- [1] M. O. Al-Kaff, H. A. El-Metwally, A. E. A. Elsadany, and E. M. Elabbasy, *Exploring chaos and bifurcation in a discrete prey-predator based on coupled logistic map*, Scientific Reports, 14(1) (2024), 16118.



- [2] L. J. Allen, *An introduction to stochastic processes with applications to biology*, CRC Press, 2010.
- [3] J. Carr, *Applications of centre manifold theory*, Vol. 35, Springer Science & Business Media, 2012.
- [4] S. Elaydi, *An introduction to difference equations*, Springer New York, New York, NY, 2005.
- [5] W. Govaerts, R. K. Ghaziani, Y. A. Kuznetsov, and H. G. Meijer, *Numerical methods for two-parameter local bifurcation analysis of maps*, SIAM J. Sci. Comput., 29(6) (2007), 2644–2667.
- [6] J. Guckenheimer, *Dynamical systems, and bifurcations of vector fields*, Appl. Math. Sci. Series, 42, 1986.
- [7] G. Iooss and D. D. Joseph, *Elementary stability and bifurcation theory*, Springer Science & Business Media, 2012.
- [8] M. Kot, *Elements of mathematical ecology*, Cambridge University Press, 2001.
- [9] Y. A. Kuznetsov, *Elements of applied bifurcation theory*, Springer New York, New York, NY, 1998.
- [10] Y. A. Kuznetsov and H. G. Meijer, *Numerical bifurcation analysis of maps*, Vol. 34, Cambridge University Press, 2019.
- [11] R. M. May, *Simple mathematical models with very complicated dynamics*, Nature, 261(5560) (1976), 459–467.
- [12] J. D. Murray, *Mathematical biology: I. An introduction*, Vol. 17, Springer Science & Business Media, 2007.
- [13] S. Wiggins, *Introduction to applied nonlinear dynamical systems and chaos*, Springer New York, New York, NY, 2003.

Uncorrected Proof

